HHS Public Access

Author manuscript

Mucosal Immunol. Author manuscript; available in PMC 2013 January 01.

Published in final edited form as:

Mucosal Immunol. 2012 July ; 5(4): 432–443. doi:10.1038/mi.2012.20.

CD8α⁺β⁻ and CD8α⁺β⁺ plasmacytoid dendritic cells induce Foxp3⁺ regulatory T cells and prevent the induction of airway hyperreactivity

Vincent Lombardi, **Anneliese O. Speak**, **Jérôme Kerzerho**, **Natacha Szely**, and **Omid Akbari**

Department of Molecular Microbiology and Immunology, Keck School of Medicine, University of Southern California, Los Angeles, California, 90033, USA

Abstract

Dendritic cells (DCs) control the balance between protection against pathogens and tolerance to innocuous or self-antigens. Here, we demonstrate for the first time that mouse plasmacytoid DCs (pDCs) can be segregated into three distinct populations, exhibiting phenotypic and functional differences, according to their surface expression of CD8α or CD8β as $CD8\alpha^{-}\beta^{-}$, $CD8\alpha^{+}\beta^{-}$ or $CD8\alpha^{+}\beta^{+}$. In a mouse model of lung inflammation, adoptive transfer of $CD8\alpha^{+}\beta^{-}$ or $CD8\alpha^{+}\beta^{+}$ pDCs prevents the development of airway hyperreactivity. The tolerogenic features of these subsets are associated with increased production of retinoic acid, which leads to the enhanced induction of $Foxp3^{+}$ regulatory T cells compared to $CD8\alpha^{-}\beta^{-}$ pDCs. Our data thus identify subsets of pDCs with potent tolerogenic functions that may contribute to the maintenance of tolerance in mucosal sites such as the lungs.

INTRODUCTION

Dendritic cells (DCs) constitute a family of cells with the unique ability to distinguish pathogens from innocuous microorganisms as well as self from non-self antigens [1, 2]. These cells can further initiate a robust immune response to infectious agents or in contrast, maintain immune tolerance to innocuous or self-antigens. To accomplish these tasks, DCs are equipped with pattern recognition receptors that recognize motifs highly conserved in pathogens throughout the evolution [3]. Engagement of these receptors triggers the up-regulation of co-stimulatory molecules and the production of immune mediators such as cytokines. Along with the capacity of DCs to present antigen, these signals direct the differentiation of naïve $CD4^{+}$ T cells into the appropriate subset of T helper (T_H) cells [2, 4, 5]. Therefore, DCs are key regulators of the immune system considering their ability to control the balance between immunity and tolerance [2, 4]. How DCs achieve these apparently

Corresponding author: Omid Akbari, Ph.D., Address: 1450 Biggy Street, NRT5505, Los Angeles, CA 90033, Fax: 323 442 7944, Phone: 323 442 7930, akbari@usc.edu.

DISCLOSURE

The authors have no conflicting financial interests.

opposite functions remains elusive and many studies suggest that immunogenic and tolerogenic functions are assigned to different subpopulations of DCs [2, 4–6].

DCs can be divided into two populations that express different cell surface markers, morphology, migratory routes and exhibit different functional properties [7]. Conventional DCs (cDCs) can be defined by their CD11c^{hi} MHC class II^{hi} phenotype whereas plasmacytoid DCs (pDCs) are identified as CD11c^{low} MHC class II^{dim} CD45R/B220^{+} BST2/mPDCA-1^{+} [8]. Increasing evidence suggests that pDCs are vital mediators of anti-viral immunity in part due to their expression of receptors specialized for the recognition of pathogen derived nucleic acids (toll like receptor (TLR) 7 and 9) and rapid release of type I interferons after activation by TLR engagement [9]. However, it is now becoming evident that pDCs are also key mediators of tolerance in mucosal sites. For example, depletion of pDCs prevents the establishment of respiratory tolerance [10] and adoptive transfer of pDCs can reduce established lung inflammation in animal models [11]. In an oral tolerance model, pDCs have been shown to be essential for the presentation of dietary antigens [12] and their role in the induction of tolerance to transplanted grafts has been suggested [13, 14]. However, all these studies have used total pDC populations and the identification or functional description of pDC subsets has not been elucidated as it has been previously described for many subsets of cDCs in the induction of tolerance. For instance, the gut-associated lymphoid tissue contains a subset of DCs, defined by expression of the mucosal integrin CD103, that have immuno-regulatory properties [15]. These cells are able to promote the differentiation of Foxp3^{+} regulatory T cells (T_{reg}) cells from naïve CD4^{+} T cells. In the lungs, under normal conditions, respiratory exposure to antigen elicits the generation of tolerogenic cDCs and Foxp3^{+} T_{reg} cells resulting in immune tolerance [16–18]. In addition to the tolerogenic function of pDCs and cDCs, mucosal tissues also contain a specialized microenvironment that is required for the induction and maintenance of tolerance. In the gut CD103^{+} DCs release retinoic acid, which increases the transforming growth factor β (TGF-β) mediated conversion of naïve CD4^{+} T cells into Foxp3^{+} T_{reg} cells [15, 19]. Retinoic acid is generated from vitamin A in a two-step process catalyzed by alcohol dehydrogenase and then retinal dehydrogenase (RALDH) and is known to be a potent immunoregulatory compound [20]. Previous studies examining the expression and activity of RALDH enzymes in DCs demonstrated that cDCs isolated from mucosal sites possess greatly enhanced RALDH activity compared to spleen cDCs [21]. A deregulation of mucosal tolerance can lead to the development of immune disorders such as allergic diseases, inflammatory bowel disease and asthma [5, 22].

Herein, we demonstrate for the first time that pDCs can express CD8α alone or in combination with CD8β and can be segregated into three subpopulations, CD8α^{-}β^{-}, CD8α^{+}β^{-} and CD8α^{+}β^{+}. These subsets of pDCs demonstrate differential cytokine secretion and functional properties both *in vitro* and *in vivo*. Adoptive transfer of CD8α^{-}β^{-} pDCs triggered sensitization when transferred into naïve mice, whereas CD8α^{+}β^{-} and CD8α^{+}β^{+} pDCs exhibited poor capacity for sensitization. In contrast using a model of airway inflammation, adoptive transfer of CD8α^{+}β^{-} and CD8α^{+}β^{+} pDCs prevents the development of airway hyperreactivity. Therefore, CD8α^{+}β^{-} or CD8α^{+}β^{+} pDCs can induce tolerance *in vivo*. One potential mechanism for this observation is the induction of T_{reg} cells. We have

discovered that CD8α$^+$β$^-$ or CD8α$^+$β$^+$ pDCs strongly support the differentiation of Foxp3$^+$ CD4$^+$ T_{reg} cells both *in vivo* and *in vitro*. The ability of tolerogenic pDC subsets to induce T_{reg} cells is associated with the increased expression of *Aldha1a1*, *Aldha1a2* and *Aldha1a3* genes encoding RALDH1, RALDH2 and RALDH3 enzymes respectively. Inhibition of RALDH activity prevents the induction of Foxp3$^+$ T_{reg} cells by CD8α$^+$β$^-$ or CD8α$^+$β$^+$ pDCs. Therefore, our data show that CD8α and CD8β can define subpopulations of pDCs, which possess either tolerogenic (CD8α$^+$β$^-$ or CD8α$^+$β$^+$) or pro-inflammatory (CD8α$^-$β$^-$) properties.

RESULTS

A subset of plasmacytoid dendritic cells express CD8α or CD8αβ

In a selection of organs (spleen, peripheral lymph nodes and lungs), we analyzed by flow cytometry the expression of an assortment of myeloid and lymphoid markers on the plasmacytoid population of DCs, in order to identify subsets of pDCs. We observed expression of CD8α and CD8β on pDCs which can define three subsets: CD8α$^-$β$^-$, CD8α$^+$β$^-$ and CD8α$^+$β$^+$ (Figure 1a). To confirm our findings by flow cytometry, we performed several staining controls (Figure S1a) and used two different clones specific for CD8β (H35-17.2 and 53-5.8) with similar results obtained with both clones (Data not shown). These findings were validated by fluorescent confocal microscopy analysis of pDCs purified from peripheral lymph nodes and stained with mPDCA1, anti-IA/IE or anti-CD11c in addition to CD8α and CD8β (Figure 1b). We showed that a subset of pDCs express CD8α alone or associated with CD8β (Figure 1b). Depending on the tissue analyzed, CD8α$^+$β$^-$ pDCs represent 10 to 22% of pDCs and CD8α$^+$β$^+$ pDCs 4 to 23% of the whole population of pDCs (Figure 1c). The three subsets of pDCs described herein exhibit all the specific markers of terminally differentiated pDCs (positive for mPDCA1, Siglec-H, Ly6C, B220 and Ly49Q) and display an immature phenotype with a low expression of co-stimulatory molecules CD40, CD80, CD86, PD-L1, PD-L2, ICOS-L and OX40-L (Figure 1d). To test whether *in vivo* expansion of DCs affects the expression of CD8α or CD8β at the surface of pDCs, Renca tumor cells expressing Fms-like tyrosine kinase 3-ligand (Flt3-L) were subcutaneously injected into BALB/c mice. Flt3-L acts on hematopoietic stem cells and controls their differentiation into DCs, this treatment expands the population of DCs by 15 to 20 fold after 14 days without activating the cells [23]. We observed that Flt3-L treatment does not significantly affect the level of expression of CD8α and CD8β on pDCs (Supplementary figure 1b). The expression of CD8α and CD8β was assessed simultaneously on pDCs (CD11c^{dim} mPDCA1$^+$ cells) and on conventional DCs (cDCs, CD11c^{high} mPDCA1$^-$ cells). At the surface of cDCs, only CD8α expression was detected (Figure S1b). To prevent any irrelevant signal coming from CD8-expressing T cells, DCs were gated on CD11c$^+$ cells while T cells were excluded in the gating strategy by CD3 staining (Figure S1b). To confirm our results, we sorted each subset by flow cytometry (cell sorting purity is presented in Figure S2a) and assessed the gene expression of *Cd8a* and *Cd8b* genes by real-time PCR. In agreement with the surface phenotype, *Cd8a* gene expression was detected in CD8α$^+$β$^-$ pDCs while both *Cd8a* and *Cd8b* genes were strongly expressed in the CD8α$^+$β$^+$ subset (Figure 2a). As expected *Cd8b* gene expression was never detected in cDCs. To examine if the surface expression of CD8α or CD8β is due to the possible uptake of CD8

antigens from $CD8^+$ T cells[24], we analyzed the expression of CD8α and CD8β in pDCs from β2 microglobulin knock out ($B2m^{-/-}$) mice. These mice lack cell surface MHC class I expression and thus $CD8^+$ T cells [25]. The pDCs from $B2m^{-/-}$ animals exhibited the same profile of CD8α and CD8β expression as wild type controls demonstrating the *bona fide* expression of these proteins by pDCs (Figure 2b). Furthermore, this was confirmed by quantitative real-time PCR after isolation of each subpopulation by cell sorting (Figure 2c). Collectively, these data confirm that pDCs express CD8α or CD8αβ and can be divided into three subsets accordingly.

$CD8\alpha^-\beta^-$, $CD8\alpha^+\beta^-$ and $CD8\alpha^+\beta^+$ pDCs present distinct cytokine production, antigen uptake and priming properties

The main function of DCs is to prime naïve T cells by presenting antigen and providing additional signals through costimulatory molecules and production of cytokines. To address whether the subsets of pDCs described herein differ in these functions, we stimulated them with TLR ligands and assessed the expression of costimulatory molecules along with the cytokine production. We stimulated $CD8\alpha^-\beta^-$, $CD8\alpha^+\beta^-$ and $CD8\alpha^+\beta^+$ pDCs with R848 (synthetic TLR7 ligand) and CpG oligonucleotides (TLR9 ligand) and assessed the production of IFN-α, TNF-α, IL-6 and IL-10. Plasmacytoid DCs are known to produce large amount of type I interferon in response to a viral infection but also reported to produce significant levels of IL-6 and IL-10 [8, 26–28]. We observed that, after activation via either TLR7 or TLR9, the expression of CD8α or CD8β is not altered and we did not detect any difference in the upregulation of costimulatory molecules between the three subsets (Data not shown). Interestingly, it appeared that $CD8\alpha^-\beta^-$ produce more IFN-α, TNF-α, IL-6 and IL-10 than $CD8\alpha^+\beta^-$ and $CD8\alpha^+\beta^+$ pDCs upon stimulation (Figure 3a) despite a similar expression of TLR7 and 9 (Data not shown). We next tested the antigen uptake capacity of the pDCs using a fluorescent antigen (ovalbumin-APC (OVA-APC)) in a flow cytometry-based assay. $CD8\alpha^+\beta^+$ pDCs have an enhanced capacity to endocytose antigen compared to $CD8\alpha^+\beta^-$ and $CD8\alpha^-\beta^-$ pDCs, which demonstrated an intermediate and low uptake capacity respectively (Figure 3b). We then explored whether the three subtypes of pDCs described in this study have a different ability to prime $CD4^+$ T cells. We performed an *in vitro* co-culture between these subsets of pDCs and $CD4^+$ T cells isolated from DO11.10 mice with an OVA-specific transgenic T cell receptor (TCR). In response to OVA, we observed a robust proliferation when $CD8\alpha^-\beta^-$ pDCs were used as the antigen presenting cells (APCs) (Figure 3c). In contrast $CD8\alpha^+\beta^-$ pDCs and $CD8\alpha^+\beta^+$ pDCs poorly supported the proliferation of $CD4^+$ T cells in response to antigen stimulation *in vitro* (Figure 3c). As expected, the production of IL-2 was correlated with the trends observed during the proliferation assay (Figure 3c). Therefore these pDC subsets segregated according to their expression of CD8α or CD8β exhibit striking differences in their capacity to trigger the proliferation of naïve $CD4^+$ T cells, to produce cytokines or to uptake antigens.

Transfer of $CD8\alpha^-\beta^-$ pDCs triggers the development of airway inflammation

As demonstrated above these pDC subsets exhibit differential ability to process and present antigens and to activate $CD4^+$ T cells *in vitro*. We therefore wanted to test the functional capacity of these pDCs subsets to confer antigen sensitization *in vivo* using a model of airway hyperreactivity (AHR). Thus, we sorted pDC subsets from mice treated with Flt3-L,

loaded them with OVA and adoptively transferred these cells or OVA-loaded bone marrow-derived DCs (BM-DCs) as a positive control, into naïve mice. Mice were challenged intranasally with antigen one week later (Figure 4a). Lung inflammation was assessed by evaluating AHR by plethysmography as well as lung histology. In agreement with the *in vitro* ability to activate T cells, adoptive transfer of $CD8\alpha^{-}\beta^{-}$ pDCs supported the robust development of AHR as determined by lung resistance (R_L) and dynamic compliance (C_{dyn}) in anesthetized, tracheotomized and ventilated animals or as enhance pause (Penh) in conscious animals (Figure 4b and c). In contrast $CD8\alpha^{+}\beta^{-}$ and $CD8\alpha^{+}\beta^{+}$ pDCs, which demonstrated poor ability to induce T cell proliferation *in vitro*, did not trigger significant AHR (Figure 4b and c). We then examined lung histology to support the lung function data. Lung sections were stained with hematoxylin and eosin (H&E) to observe cellular infiltration or periodic acid Schiff (PAS) to examine mucus production. In accordance with the plethysmography results, a massive cell infiltration as well as significant mucus production was observed in mice transferred with $CD8\alpha^{-}\beta^{-}$ pDCs (Figure 4d). In contrast, only minor cellular infiltration and no mucus secretion was observed after transfer of $CD8\alpha^{+}\beta^{-}$ pDCs, while lungs of mice that received $CD8\alpha^{+}\beta^{+}$ pDCs did not present considerable abnormalities (Figure 4d). These results collectively show that $CD8\alpha^{-}\beta^{-}$ pDCs can be considered as an immunogenic population of pDCs in contrast with $CD8\alpha^{+}\beta^{-}$ or $CD8\alpha^{+}\beta^{+}$ pDCs.

$CD8\alpha^{+}\beta$ or $CD8\alpha^{+}\beta^{+}$ pDCs prevents AHR and inflammation

As $CD8\alpha^{+}\beta^{-}$ and $CD8\alpha^{+}\beta^{+}$ pDCs subsets demonstrated poor immunogenic capacity *in vitro* and *in vivo* we hypothesized that these subsets may exhibit tolerogenic properties *in vivo*. To examine this possibility, the three subsets of pDCs were initially loaded with OVA and adoptively transferred to naïve mice that were subsequently sensitized and challenged (Figure 5a). We observed that respiratory function of mice transferred with $CD8\alpha^{+}\beta^{-}$ pDCs and more especially $CD8\alpha^{+}\beta^{+}$ pDCs were significantly improved (Figure 5b). In contrast, animals that received $CD8\alpha^{-}\beta^{-}$ pDCs demonstrated a robust induction of AHR that was indistinguishable to the positive control group (mice that received saline solution) (Figure 5b). Accordingly, analysis of lung histology showed that only mice treated with $CD8\alpha^{-}\beta^{-}$ pDCs exhibited a high cellular infiltration and mucus secretion characteristic of airway inflammation (Figure 5c). We also demonstrated that in mice treated with either $CD8\alpha^{+}\beta^{-}$ or $CD8\alpha^{+}\beta^{-}$ pDCs the production of T_H2 cytokines IL-4 and IL-13 is reduced significantly compared to sensitized mice (Figure 5d). Similarly, levels of OVA-specific IgG and IgE were diminished in mice, which received either $CD8\alpha^{+}\beta^{-}$ or $CD8\alpha^{+}\beta^{-}$ pDCs (Figure 5e). Therefore, $CD8\alpha^{+}\beta^{+}$ and $CD8\alpha^{+}\beta^{-}$ pDCs promote the development of immune tolerance as shown by their ability to prevent lung inflammation and can therefore be classified as *bona fide* tolerogenic pDC subsets.

$CD8\alpha^{+}\beta^{-}$ and $CD8\alpha^{+}\beta^{+}$ pDCs promote the differentiation of antigen-specific $CD4^{+}$ $CD25^{+}$ $Foxp3^{+}$ T cells *in vivo*

Tolerance may be achieved by multiple mechanisms, including induction of $Foxp3^{+}$ T_{reg} cells, which suppress the activity of antigen specific effector T cells [29]. We therefore sought to determine the mechanism that allows $CD8\alpha^{+}\beta^{-}$ and CD8 $\alpha^{+}\beta^{+}$ pDCs to induce T cell tolerance *in vivo*. To test the ability of these pDC subsets to induce the conversion of naïve

$CD4^+$ T cells into $Foxp3^+$ T_{reg} cells, we performed an *in vivo* adoptive transfer study. We co-transferred naïve **$CD4^+$ $CD62L^+$ $Foxp3^-$** T cells isolated from OVA-specific DO11.10 mice with the different OVA-loaded pDC subsets into naïve mice (purity of naïve $CD4^+$ T cells Figure S2c and S2d). After four days, we challenged the mice intranasally with OVA in order to recruit T cells to the lungs and then analyzed Foxp3 expression in the spleen and lungs by flow cytometry. We tracked the conversion of OVA-specific $CD4^+$ T cells into Foxp3-expressing cells using the clonotypic antibody KJ1.26 specific of the OVA-specific transgenic TCR [30] (Figure 6a). The percentage of $CD4^+$ $KJ1.26^+$ $CD25^+$ $Foxp3^+$ T cells was significantly increased in mice that received $CD8\alpha^+\beta^-$ or $CD8\alpha^+\beta^+$ pDCs (Figure 6b). With the transfer of this last subset, the percentage of $CD4^+$ $CD25^+$ $Foxp3^+$ T cells was increased by two fold in the lungs compared to transfer of $CD8\alpha^-\beta^-$ pDCs. Therefore, $CD8\alpha^+\beta^-$ and $CD8\alpha^+\beta^+$ pDCs possess the capacity to induce antigen-specific $CD4^+$ $CD25^+$ $Foxp3^+$ T_{reg} cells *in vivo*.

RALDH expression in $CD8\alpha^+\beta^-$ or $CD8\alpha^+\beta^+$ pDCs is responsible for induction of Tregs

The induction of T_{reg} cells *in vivo* by tolerogenic DCs has previously been demonstrated to be regulated by TGF-β and retinoic acid [31]. To test the role of retinoic acid we analyzed the gene expression of the aldehyde dehydrogenase enzymes (RALDH) that catalyze one step of the conversion of retinol into retinoic acid. We determined that *Aldha1a1*, *Aldha1a2* and *Aldha1a3*, three genes encoding RALDH1, RALDH2 and RALDH3 enzymes respectively, were up-regulated in the tolerogenic $CD8\alpha^+\beta^-$ or $CD8\alpha^+\beta^+$ pDC subsets (Figure 7a). As a control, we tested simultaneously the expression of these genes in $CD103^+$ cDCs from mesenteric lymph nodes that have previously been demonstrated to induce $Foxp3^+$ T_{reg} cells in a retinoic acid dependent manner [15, 19]. In accordance with previous reports $CD103^+$ cDCs expressed high levels of *Aldha1a1* and *Aldha1a2* compared to $CD103^-$ cDCs but did not express *Aldh1a3* in contrast to the pDC subsets described herein (Figure 7a). In order to demonstrate the functional activity of RALDH in pDCs we used the fluorescent RALDH substrate, Aldefluor, in a flow cytometry assay, as has been previously demonstrated [21, 32]. In agreement with the hierarchy of T_{reg} induction capacity *in vivo* and *Aldha* genes expression, $CD8\alpha^+\beta^+$ pDC demonstrated the highest RALDH activity and $CD8\alpha^-\beta^-$ the lowest (Figure 7b). We next tested the requirements for TGF-β and retinoic acid in the conversion of naïve T cells into T_{reg} cells by pDC subsets *in vitro*. We cultured pDC subsets with naïve OVA-specific $CD4^+$ T cells in the presence or absence of TGF-β or TGF-β and RALDH inhibitor (LE540) [31, 33]. We observed that, in presence of TGF-β, $CD8\alpha^+\beta^+$ and $CD8\alpha^+\beta^-$ pDCs are more efficient in converting naïve $CD4^+$ T cells into Foxp3-$\alpha^-\beta^-$ pDCs (Figure 7c). In addition, the presence of a expressing T_{reg} cells compared to CD8 RALDH inhibitor completely blocked the conversion of naïve $CD4^+$ T cells by $CD8\alpha^+\beta^+$ and $CD8\alpha^+\beta^-$ pDCs (Figure 7c). Altogether, these results demonstrate that $CD8\alpha^+\beta^-$ pDCs and in particular $CD8\alpha^+\beta^+$ pDCs strongly support the development of $Foxp3^+$ $CD4^+$ T_{reg} cells in a TGF-β and retinoic acid dependent manner.

DISCUSSION

In this study, we demonstrate for the first time that pDCs can express either CD8α or co-express CD8α and CD8β thus defining three populations of pDCs: $CD8\alpha^-\beta^-$, $CD8\alpha^+\beta^-$ and

CD8α$^+$β$^+$. These subsets express all the markers characteristic of terminally differentiated immature pDCs and possess a similar expression of co-stimulatory molecules. However, these three pDC subsets exhibited striking differences in their functional capacity to uptake antigen, produce cytokines after activation and prime naïve CD4$^+$ T cells. Furthermore, we have determined *in vivo* that CD8α$^-$β$^-$ pDCs are immunogenic whereas CD8α$^+$β$^-$ and CD8α$^+$β$^+$ pDCs exhibited tolerogenic properties. This is associated with the ability of CD8α$^+$β$^-$ and CD8α$^+$β$^+$ pDCs to support very effectively the conversion of naïve CD4$^+$ T cells into Foxp3$^+$ T_{reg} cells both *in vivo* and *in vitro*. Tolerogenic subsets of pDCs express three isoforms of RALDH enzymes and blocking the activity of these enzymes was shown to be essential for this conversion to occur. Our findings thus suggest that the expression of CD8α or CD8αβ by pDCs define three subsets of cells exhibiting different functions and that CD8α$^+$β$^-$ and CD8α$^+$β$^+$ pDCs demonstrate *bona fide* tolerogenic properties.

There is strong evidence that pDCs have critical roles in induction of peripheral tolerance. For example pDCs are essential to maintain tolerance in the lungs [10, 11] and digestive tract [12]. In addition, pDCs have been shown to offer therapeutic benefit in murine models of graft versus host disease [13, 14] and lung inflammation [10]. Induction of tolerance is important in mucosal tissues in terms of immune responses to antigens encountered in the respiratory and intestinal tracts. These sites are continuously exposed to a wide variety of environmental, nonpathogenic antigens, which induce immune tolerance or hyporesponsiveness rather than active immunity [34, 35]. Thus, under normal circumstances, food allergen in the intestinal tract or inhaled allergens in the airways generally do not induce protective immune responses. However, in individuals with allergic asthma, processing of these proteins result in the induction of antigen-specific T_H2-biased inflammatory responses that cause AHR and asthma [5]. The specific events that alter antigen processing and presentation in the lungs of these individuals who have allergic asthma and that abrogate tolerance are not yet clear, but we suggest that tolerogenic pDC repertoire and/or function in these individuals might be altered. Acting on population of tolerogenic dendritic cells such as CD8α$^+$β$^-$ and CD8α$^+$β$^+$ pDCs capable to induce antigen-specific regulatory T cell can restore immune tolerance to allergens. As a result, the identification of cells with tolerogenic functions is of great interest for the design of interventional approaches to control disorders related to an imbalance in immunological tolerance such as allergy and autoimmune diseases.

Only few reports described subpopulation of pDCs. For instance, CCR9 and CD9 expression were shown to define subsets of murine pDCs [13, 36]. However, CCR9$^-$ and CD9$^+$ pDCs do not display all the specific markers of terminally differentiated pDCs in contrast with the three subsets of pDCs described in this study. Interestingly, CCR9$^+$ pDCs exhibit tolerogenic properties *in vitro* and *in vivo* [13] but we determined by flow cytometry that either the immunogenic (CD8α$^-$β$^-$) or the tolerogenic subsets (CD8α$^+$β$^-$ and CD8α$^+$β$^-$) of pDCs we have described, express comparable levels of CCR9 (Data not shown). Another difference is that CCR9$^+$ pDCs downregulate CCR9 after activation with TLR ligands whereas, the pDCs subsets we have defined according to CD8α and CD8β expression are not altered after TLR engagement. CD8α was originally reported in mice to be expressed on a subset of cDCs characterized by their ability to produce high quantities of IL-12, to

capture dead cells and to cross-present antigens [37]. Our data reveal that mouse pDCs can not only express CD8α but also CD8β. Both cDCs and pDCs expressing CD8α share several properties such as strong antigen uptake ability, weak capacity to prime $CD4^+$ T cells as well as tolerogenic features [38, 39]. However, the functional human counterpart of mouse $CD8\alpha^+$ cDCs recently described to express CD141 (BDCA3) do not display a plasmacytoid phenotype [40–43]. In order to translate our findings to human, further investigations are required to identify markers defining the human equivalent of mouse $CD8\alpha^+\beta^-$ and $CD8\alpha^+\beta^+$ pDCs.

Expression of *Aldh* genes was greatly increased in tolerogenic $CD8\alpha^+\beta^-$ and $CD8\alpha^+\beta^+$ pDC subsets and correlated with RALDH activity as determined with a fluorescent substrate, Aldefluor, by flow cytometry. It has previously been demonstrated that RALDH activity in specific subsets of APCs is increased at mucosal sites [15, 20, 21, 44, 45]. This is thought to be associated with the requirement for the induction of tolerance at these sites due to the constant exposure to innocuous antigens. In mucosal APCs, expression of RALDH and the subsequent production of retinoic acid are vital for the induction of T cell tolerance and induction of T_{reg} cells [15, 31]. Interestingly, tolerogenic cDCs from the gut express only two isoforms of RALDH (RALDH1 and 2) [44–46], whereas the tolerogenic pDCs susbets reported herein have increased expression of RALDH3 in addition to RALDH1 and 2. The expression of RALDH3 in tolerogenic subsets of APCs was not reported earlier suggesting that all the enzymes involved in the biosynthesis of retinoic acid can be considered as a suitable marker of DCs with the ability to promote the generation of $Foxp3^+$ $CD4^+$ T cells. When we inhibited RALDH activity *in vitro*, the capacity of tolerogenic pDCs to induce conversion on naïve $CD4^+$ T cells into $Foxp3^+$ T_{reg} cells was greatly diminished. Therefore, targeting RALDH activity would allow for the manipulation of tolerance induction by pDCs in allergic diseases, autoimmunity or in repression of immunological tolerance to cancer cells.

In conclusion, here we have used several molecular and cellular approaches, to segregate tolerogenic pDCs from other DCs. We have shown that the expression of CD8α and in particular CD8α and CD8β designate new subsets of tolerogenic pDCs with the capacity to induce the differentiation of $Foxp3^+$ T_{reg} cells and are very effective in suppressing AHR. The induction of T_{reg} cells was dependent on retinoic acid and TGF-β. Therefore, strategies to expand or activate tolerogenic pDC subsets might therefore have an important role in the induction and maintenance of peripheral tolerance. Thus, future studies to explore the possibility of targeting tolerogenic pDC subsets *in vivo* in order to use them for therapeutic purposes will benefit a wide range of inflammatory disorders, including autoimmunity, allergic disorders and transplantation.

METHODS

Mice

Female BALB/c ByJ mice and B6(Cg)-Tg(B2M)1Trg Tg(HLA-B)1Trg/Dcr ($B2m^{-/-}$) mice (all 6 to 8 weeks old) were purchased from The Jackson Laboratory (Bar Harbor, ME). All mice were maintained in a pathogen-free mouse colony at the Keck School of Medicine

(University of Southern California) under protocols approved by the Institutional Animal Care and Use Committee.

Flow cytometry

Cells were pre-incubated with normal rat serum and washed before staining. Subsets of dendritic cells were identified using various antibody combinations including anti-B220 APC-Cy7 (RA3-6B2), anti-CD40 FITC (3/23), anti-CD80 (16-10A1), anti-CD86 PerCP-Cy5.5 (GL1), anti-IA/IE (M5/114.15.2), anti-Ly6c PerCP-Cy5.5 (HK1.4), anti-CD8α PE-Cy7 (53-6.7), anti-CD8β APC (H35-17.2 or 53-5.8), anti-CD3 PerCP-Cy5.5 (145-2C11), anti-PD-L1 (MIH5, all from BD Biosciences, San Jose, CA), Siglec-H (eBio440c), anti-ICOS-L (HK5.3), anti-CD11c eFluor450 (N418), anti-PD-L2 (122, all from eBioscience, San Diego, CA), anti-mPDCA1 PE (Miltenyi Biotec, Auburn, CA) and anti-Ly49Q (2E6, MBL International, Woburn, MA). The cells were washed with cold PBS + 2% fetal calf serum and acquired with an 8-color FACS Canto II flow cytometer (BD Biosciences). The data were analyzed using FlowJo 6.2 software (Tree Star, Ashland, OR).

Plasmacytoid DC isolation and cells sorting

To prepare single cell suspension, peripheral lymph nodes (cervical and inguinal lymph nodes pooled) were digested with 1.6 mg/ml collagenase (CLS4, Worthington Biochemicals, Lakewood New Jersey) and 0.1% DNAse I (Fraction IX, Sigma, St. Louis, Missouri) at 37°C on an orbital shaker for 15 minutes, and for an additional 15 minutes after passing it multiple times through an 18 gauge needle. For *in vivo* expansion of DCs, we prepared Renca (BALB/c renal carcinoma cell line) cells expressing Flt3-L [23, 47, 48] and subcutaneously injected 5×10^6 cells into BALB/c mice. For $B2m^{-/-}$ mice, we used B16 melanoma expressing Flt3-L as previously described[23]. After 14 days, peripheral lymph nodes were harvested and processed as described above. To isolate pDCs, cells were labeled with anti-mPDCA-1 microbeads (Miltenyi) and then positively sorted by AutoMACS according to the manufacturer's instruction. Purity of pDCs was always greater than 95%. Plasmacytoid DC subsets were identified based on CD11c and mPDCA1 staining; $CD8\alpha^-\beta^-$, $CD8\alpha^+\beta^-$ and $CD8\alpha^+\beta^+$ pDC subsets were sorted using a FACS ARIA III cell sorter (BD Biosciences).

Confocal microscopy

Plasmacytoid DCs were sorted as described above and cells were stained for surface markers with the following antibodies: anti-CD8α Cy5 (53–6.7), anti-CD8β TRITC (H35-17.2, both from eBioscience) and either anti-IA/IE (M5/114.15.2), anti-CD11c (HL3, all from BD Bioscience) or mPDCA1 (Miltenyi) antibodies conjugated to FITC. Cells were subsequently fixed and permeabilized using the BD Biosciences Fix/Perm solution. Washed cells were mounted onto slides in Vectashield mounting medium (Vector Laboratories, Burlingame, CA). Images were acquired with a Nikon Eclipse Ti confocal microscope (Nikon, Instruments, Melville, NY) using a 100x oil objective associated to the Nikon EC-Z1 software.

Quantitative real-time PCR

Total RNA was extracted from sorted subtypes of pDCs using the RNAasy mini kit (Qiagen, Valencia, CA) and cDNAs were generated with the High Capacity cDNA Reverse Transcription Kit (Applied Biosystems, Carlsbad, CA) according to the manufacturer's recommendations. Quantification of mRNA levels was carried out by quantitative real-time PCR on a CFX96 thermal cycler (Bio-Rad, Hercules, CA) with predesigned Taqman gene expression assays for (*Actb*: Mm0060732_m1, *Cd8a*: Mm01182108_m1, *Cd8b*: Mm00438116_m1, *Aldh1a1*: Mm00657317_m1, *Aldh1a2*: Mm00657317_m1, *Aldh1a3*: Mm00474049_m1; Applied Biosystems, Foster City, CA) and reagents, as per manufacturer's instructions. Results were analyzed using the comparative C(T) method ($2^{-\Delta\Delta C(T)}$ method) [49].

Sensitization and tolerance models and measurement of airway responsiveness

$CD8\alpha^{-}\beta^{-}$, $CD8\alpha^{+}\beta^{-}$ and $CD8\alpha^{+}\beta^{+}$ purified pDCs were isolated from pooled peripheral lymph nodes of BALB/mice treated with Flt3-L-producing cells. Each subset was loaded with OVA (10 μg/ml) for 4 hours at 37°C. Cells were subsequently washed two times and resuspended in saline solution. For the sensitization model, 2×10^5 cells (pDCs or Bone marrow-derived DCs prepared as previously described [50]) were adoptively transferred by intravenous injection through the tail vein. Seven days after the transfer, mice were challenged on three consecutive days by intranasal administration of OVA (50 μg in PBS). For the tolerance model, OVA-loaded pDC subsets were adoptively transferred 7 days prior intraperitoneal injection of OVA (50 μg) in aluminum hydroxide (Alum, 2 mg), subsequently recipients were challenged intranasally with 3 consecutive doses of OVA (50 μg in PBS) on days 14, 15 and 16. Airway hyperesponsiveness (AHR) responses was subsequently assessed by methacholine-induced airflow obstruction in conscious mice placed in a whole-body plethysmograph (Buxco Electronics, Troy, NY) as described before [51] or by invasive measurement of airway resistance, in which anesthetized and tracheostomized mice were mechanically ventilated [52]. Briefly, aerosolized methacholine was administered in increasing concentrations of methacholine (0, 1.25, 2.5, 5 and 10 mg/ml) and we continuously computed the lungs resistance and dynamic compliance by fitting flow, volume, and pressure to an equation of motion. AHR was measured at 24 hours after the last intranasal challenge. Alternatively, sera were isolated to test OVA-specific IgE and IgG levels by ELISA (MD Bioproducts, St Paul, MN and My Biosource, San Diego, CA respectively).

Lung histology

Transcardial perfusion of lungs was performed with cold PBS and subsequently lungs were harvested for histology and fixed with 4% paraformaldehyde buffered in PBS. After fixation, the lungs were embedded in paraffin, cut into 4 μm sections and stained with H&E and PAS according to standard procedures. Histology pictures were acquired using a DFC290 Leica camera (Leica Microsystems, Bannockburn, IL).

Analysis of RALDH activity by flow cytometry

The activity of RALDH enzymes was determined using the Aldefluor staining kit (StemCell Technologies, Vancouver, Canada). Plasmacytoid DCs were isolated from pooled peripheral lymph nodes and incubated for 45 minutes at 37°C in presence of different dilution of BODIPY-aminoacetaldehyde diethyl acetal (Aldefluor substrate) with or without RALDH inhibitor DEAB. Cells were subsequently stained for mPDCA1, CD11c, CD8α and CD8β and analyzed by flow cytometry.

In vitro culture

Sorted subpopulation of pDCs were cultured for 24 hours in presence of CpG 1826 (1 μM, Invivogen, San Diego, CA), R848 (1 μg/ml, Alexis Biochemicals, San Diego, CA) or medium only. Supernatants were then harvested for further measurement of cytokine production by ELISA for IFN-α (PBL Interferon Source, Piscataway, NJ), IL-6, TNF-α and IL-10 (eBioscience). Alternatively, to test the antigen uptake capacity of pDC subsets, pDCs were incubated with OVA-APC (Invitrogen, Carlsbad, CA) for 60, 120 or 180 minutes at 4°C or 37°C then analyzed by flow cytometry. To test the ability of pDC subpopulations to prime naïve $CD4^+$ T cells, $CD8\alpha^-\beta^-$ pDCs, $CD8\alpha^+\beta^-$ pDCs and $CD8\alpha^+\beta^+$ pDCs were co-cultured with naïve $CD4^+$ T cells from DO11.10 mice in presence of OVA (10 μg) for three days at a 1:10 ratio (1×10^4 pDCs/1×10^5 T cells) in a 96-well round bottom plate. Naïve $CD4^+$ T cells were purified from spleen of DO11.10 mice using the $CD4^+$ $CD62L^+$ T Cell Isolation Kit II (Miltenyi) following the manufacturer's recommendations. The purity of sorted naïve $CD4^+$ T cells was consistently above 95%. Cells were then pulsed with tritiated thymidine (1 μCi per well) for 18 hours and proliferation was evaluated using a beta-counter (Beckman Coulter, Brea, CA) as described earlier [1]. Alternatively, supernatant were harvested to measure IL-2 production by ELISA (eBioscience). To evaluate the production of Th2 cytokines in lungs of OVA-Alum-sensitized mice treated with the different pDC subsets, a single cell suspension was prepared from lungs as previously described[53]. From this cell suspension, leukocytes were positively sorted using CD45 microbeads (Miltenyi). $CD45^+$ cells were then plated in a 96-well plate round bottom (2×10^5 cells per well) and restimulated for three days with OVA (100 μg/ml). Supernatants were harvested and tested for IL-4 and IL-13 by ELISA (eBioscience). To assess induction of Foxp3 in naïve $CD4^+$ T cells, pDC subsets were co-cultured with naïve $CD4^+$ $CD62L^+$ $Foxp3^-$ T cells isolated from DO11.10 mice at a 1:10 ratio (1×10^4 pDCs/1×10^5 T cells) in a 96-well round bottom plate. Medium was supplemented with OVA peptide ($OVA_{323\text{-}339}$, 1 μg/ml, Peptides International, Louisville, KY), anti-IL-12 (C17.8), anti-IL-4 (11.B11), anti-IFN-γ (XMG1.2) and anti-IL-6 (MP5-20F3) antibodies (all at 10 μg/ml, Bioxcell, West Lebanon, NH), with TGF-β (1 ng/ml, eBioscience) and/or LE540 (1 μM, Waco Chemicals, Richmond, VA). After five days of culture, cells were harvested, washed and stained to assess Foxp3 expression using the FJK-16s Foxp3-specific clone (eBioscience) and the Foxp3 Staining Buffet Set (eBioscience) according to the manufacturer's instructions.

Induction of antigen-specific $Foxp3^+$ T cells by pDC subsets *in vivo*

In order to test the ability of pDC subsets to generate $Foxp3^+$ T cells *in vivo*, OVA-loaded $CD8\alpha^-\beta^-$, $CD8\alpha^+\beta^-$ or $CD8\alpha^+\beta^+$ purified pDCs were adoptively transferred along with

naïve OVA-specific $CD4^+$ T cells as mentioned above (3×10^5 pDCs and 3×10^6 $CD4^+$ $CD62L^+$ $Foxp3^-$ T cells) into naïve BALB/c mice. Mice were challenged at day 4 by intranasal administration of OVA (50 μg in PBS) and sacrificed the following day. Expression of Foxp3 was evaluated by flow cytometry in $CD3^+$ $CD4^+$ $KJ1.26^+$ $CD25^+$ T cells from spleen and lungs.

Statistical analysis

Differences between groups were analyzed by two-tailed, unpaired, Student's t-test and considered significant when the p value was less than 0.05.

Supplementary Material

Refer to Web version on PubMed Central for supplementary material.

Acknowledgments

This work was supported by the NIH R01 AI066020 grant. Vincent Lombardi is supported by a Senior Research Training Fellowship from the American Lung Association.

References

1. Akbari O, DeKruyff RH, Umetsu DT. Pulmonary dendritic cells producing IL-10 mediate tolerance induced by respiratory exposure to antigen. Nat Immunol. 2001; 2:725–731. [PubMed: 11477409]
2. Coquerelle C, Moser M. DC subsets in positive and negative regulation of immunity. Immunol Rev. 2010; 234:317–334. [PubMed: 20193028]
3. Medzhitov R, Janeway CA Jr. Decoding the patterns of self and nonself by the innate immune system. Science. 2002; 296:298–300. [PubMed: 11951031]
4. Palucka K, Banchereau J, Mellman I. Designing vaccines based on biology of human dendritic cell subsets. Immunity. 2010; 33:464–478. [PubMed: 21029958]
5. Pulendran B, Tang H, Manicassamy S. Programming dendritic cells to induce T(H)2 and tolerogenic responses. Nat Immunol. 2010; 11:647–655. [PubMed: 20644570]
6. Steinman RM, Hawiger D, Nussenzweig MC. Tolerogenic dendritic cells. Annu Rev Immunol. 2003; 21:685–711. [PubMed: 12615891]
7. Shortman K, Liu YJ. Mouse and human dendritic cell subtypes. Nat Rev Immunol. 2002; 2:151–161. [PubMed: 11913066]
8. Colonna M, Trinchieri G, Liu YJ. Plasmacytoid dendritic cells in immunity. Nat Immunol. 2004; 5:1219–1226. [PubMed: 15549123]
9. Gilliet M, Cao W, Liu YJ. Plasmacytoid dendritic cells: sensing nucleic acids in viral infection and autoimmune diseases. Nat Rev Immunol. 2008; 8:594–606. [PubMed: 18641647]
10. de Heer HJ, et al. Essential role of lung plasmacytoid dendritic cells in preventing asthmatic reactions to harmless inhaled antigen. J Exp Med. 2004; 200:89–98. [PubMed: 15238608]
11. Kool M, et al. An anti-inflammatory role for plasmacytoid dendritic cells in allergic airway inflammation. J Immunol. 2009; 183:1074–1082. [PubMed: 19553531]
12. Goubier A, et al. Plasmacytoid dendritic cells mediate oral tolerance. Immunity. 2008; 29:464–475. [PubMed: 18789731]
13. Hadeiba H, et al. CCR9 expression defines tolerogenic plasmacytoid dendritic cells able to suppress acute graft-versus-host disease. Nat Immunol. 2008; 9:1253–1260. [PubMed: 18836452]
14. Ochando JC, et al. Alloantigen-presenting plasmacytoid dendritic cells mediate tolerance to vascularized grafts. Nat Immunol. 2006; 7:652–662. [PubMed: 16633346]

15. Coombes JL, et al. A functionally specialized population of mucosal CD103+ DCs induces Foxp3+ regulatory T cells via a TGF-beta and retinoic acid-dependent mechanism. J Exp Med. 2007; 204:1757–1764. [PubMed: 17620361]
16. Akbari O, et al. Antigen-specific regulatory T cells develop via the ICOS-ICOS-ligand pathway and inhibit allergen-induced airway hyperreactivity. Nat Med. 2002; 8:1024–1032. [PubMed: 12145647]
17. Lloyd CM, Murdoch JR. Tolerizing allergic responses in the lung. Mucosal Immunol. 2010; 3:334–344. [PubMed: 20505664]
18. Stock P, et al. Induction of T helper type 1-like regulatory cells that express Foxp3 and protect against airway hyper-reactivity. Nat Immunol. 2004; 5:1149–1156. [PubMed: 15448689]
19. Sun CM, et al. Small intestine lamina propria dendritic cells promote de novo generation of Foxp3 T reg cells via retinoic acid. J Exp Med. 2007; 204:1775–1785. [PubMed: 17620362]
20. Manicassamy S, Pulendran B. Retinoic acid-dependent regulation of immune responses by dendritic cells and macrophages. Semin Immunol. 2009; 21:22–27. [PubMed: 18778953]
21. Guilliams M, et al. Skin-draining lymph nodes contain dermis-derived CD103(−) dendritic cells that constitutively produce retinoic acid and induce Foxp3(+) regulatory T cells. Blood. 2010; 115:1958–1968. [PubMed: 20068222]
22. Hammad H, et al. Inflammatory dendritic cells--not basophils--are necessary and sufficient for induction of Th2 immunity to inhaled house dust mite allergen. J Exp Med. 2010; 207:2097–2111. [PubMed: 20819925]
23. Mach N, et al. Differences in dendritic cells stimulated in vivo by tumors engineered to secrete granulocyte-macrophage colony-stimulating factor or Flt3-ligand. Cancer Res. 2000; 60:3239–3246. [PubMed: 10866317]
24. Vremec D, Pooley J, Hochrein H, Wu L, Shortman K. CD4 and CD8 expression by dendritic cell subtypes in mouse thymus and spleen. J Immunol. 2000; 164:2978–2986. [PubMed: 10706685]
25. Koller BH, Marrack P, Kappler JW, Smithies O. Normal development of mice deficient in beta 2M, MHC class I proteins, and CD8+ T cells. 1990. J Immunol. 2010; 184:4592–4595. [PubMed: 20410496]
26. Hochrein H, O'Keeffe M, Wagner H. Human and mouse plasmacytoid dendritic cells. Hum Immunol. 2002; 63:1103–1110. [PubMed: 12480253]
27. Konieczna P, et al. Bifidobacterium infantis 35624 administration induces Foxp3 T regulatory cells in human peripheral blood: potential role for myeloid and plasmacytoid dendritic cells. Gut. 2011
28. Tokita D, et al. Poor allostimulatory function of liver plasmacytoid DC is associated with pro-apoptotic activity, dependent on regulatory T cells. J Hepatol. 2008; 49:1008–1018. [PubMed: 18926588]
29. Sakaguchi S, Wing K, Onishi Y, Prieto-Martin P, Yamaguchi T. Regulatory T cells: how do they suppress immune responses? Int Immunol. 2009; 21:1105–1111. [PubMed: 19737784]
30. Haskins K, et al. The major histocompatibility complex-restricted antigen receptor on T cells. I. Isolation with a monoclonal antibody. J Exp Med. 1983; 157:1149–1169. [PubMed: 6601175]
31. Mucida D, et al. Reciprocal TH17 and regulatory T cell differentiation mediated by retinoic acid. Science. 2007; 317:256–260. [PubMed: 17569825]
32. Stock A, Booth S, Cerundolo V. Prostaglandin E2 suppresses the differentiation of retinoic acid-producing dendritic cells in mice and humans. J Exp Med. 2011; 208:761–773. [PubMed: 21444662]
33. Li Y, Hashimoto Y, Agadir A, Kagechika H, Zhang X. Identification of a novel class of retinoic acid receptor beta-selective retinoid antagonists and their inhibitory effects on AP-1 activity and retinoic acid-induced apoptosis in human breast cancer cells. J Biol Chem. 1999; 274:15360–15366. [PubMed: 10336422]
34. Izcue A, Coombes JL, Powrie F. Regulatory T cells suppress systemic and mucosal immune activation to control intestinal inflammation. Immunol Rev. 2006; 212:256–271. [PubMed: 16903919]
35. Lambrecht BN, Hammad H. The role of dendritic and epithelial cells as master regulators of allergic airway inflammation. Lancet. 2010; 376:835–843. [PubMed: 20816550]

36. Bjorck P, Leong HX, Engleman EG. Plasmacytoid dendritic cell dichotomy: identification of IFN-alpha producing cells as a phenotypically and functionally distinct subset. J Immunol. 2011; 186:1477–1485. [PubMed: 21172865]
37. Villadangos JA, Shortman K. Found in translation: the human equivalent of mouse CD8+ dendritic cells. J Exp Med. 2010; 207:1131–1134. [PubMed: 20513744]
38. Shortman K, Heath WR. The CD8+ dendritic cell subset. Immunol Rev. 2010; 234:18–31. [PubMed: 20193009]
39. Wang L, et al. Programmed death 1 ligand signaling regulates the generation of adaptive Foxp3+CD4+ regulatory T cells. Proc Natl Acad Sci U S A. 2008; 105:9331–9336. [PubMed: 18599457]
40. Bachem A, et al. Superior antigen cross-presentation and XCR1 expression define human CD11c +CD141+ cells as homologues of mouse CD8+ dendritic cells. J Exp Med. 2010; 207:1273–1281. [PubMed: 20479115]
41. Contreras V, et al. Existence of CD8alpha-like dendritic cells with a conserved functional specialization and a common molecular signature in distant mammalian species. J Immunol. 2010; 185:3313–3325. [PubMed: 20702727]
42. Jongbloed SL, et al. Human CD141+ (BDCA-3)+ dendritic cells (DCs) represent a unique myeloid DC subset that cross-presents necrotic cell antigens. J Exp Med. 2010; 207:1247–1260. [PubMed: 20479116]
43. Poulin LF, et al. Characterization of human DNGR-1+ BDCA3+ leukocytes as putative equivalents of mouse CD8alpha+ dendritic cells. J Exp Med. 2010; 207:1261–1271. [PubMed: 20479117]
44. Denning TL, Wang YC, Patel SR, Williams IR, Pulendran B. Lamina propria macrophages and dendritic cells differentially induce regulatory and interleukin 17-producing T cell responses. Nat Immunol. 2007; 8:1086–1094. [PubMed: 17873879]
45. Manicassamy S, et al. Activation of beta-catenin in dendritic cells regulates immunity versus tolerance in the intestine. Science. 2010; 329:849–853. [PubMed: 20705860]
46. Molenaar R, et al. Expression of retinaldehyde dehydrogenase enzymes in mucosal dendritic cells and gut-draining lymph node stromal cells is controlled by dietary vitamin A. J Immunol. 2011; 186:1934–1942. [PubMed: 21220692]
47. Lyman SD, et al. Molecular cloning of a ligand for the flt3/flk-2 tyrosine kinase receptor: a proliferative factor for primitive hematopoietic cells. Cell. 1993; 75:1157–1167. [PubMed: 7505204]
48. Murphy GP, Hrushesky WJ. A murine renal cell carcinoma. J Natl Cancer Inst. 1973; 50:1013–1025. [PubMed: 4703766]
49. Schmittgen TD, Livak KJ. Analyzing real-time PCR data by the comparative C(T) method. Nat Protoc. 2008; 3:1101–1108. [PubMed: 18546601]
50. Inaba K, et al. Generation of large numbers of dendritic cells from mouse bone marrow cultures supplemented with granulocyte/macrophage colony-stimulating factor. J Exp Med. 1992; 176:1693–1702. [PubMed: 1460426]
51. Akbari O, et al. Essential role of NKT cells producing IL-4 and IL-13 in the development of allergen-induced airway hyperreactivity. Nat Med. 2003; 9:582–588. [PubMed: 12669034]
52. Akbari O, et al. ICOS/ICOSL interaction is required for CD4+ invariant NKT cell function and homeostatic survival. J Immunol. 2008; 180:5448–5456. [PubMed: 18390727]
53. Stock P, Lombardi V, Kohlrautz V, Akbari O. Induction of airway hyperreactivity by IL-25 is dependent on a subset of invariant NKT cells expressing IL-17RB. J Immunol. 2009; 182:5116–5122. [PubMed: 19342692]

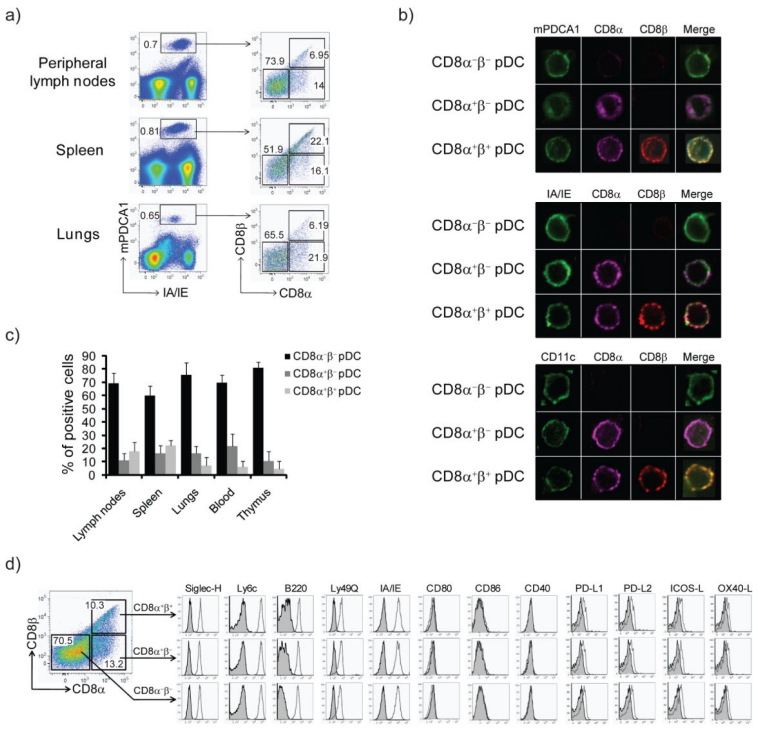

Figure 1. Plasmacytoid DCs express either CD8α or CD8αβ

(a) Cells prepared from peripheral lymph nodes, spleen or lungs of naïve mice were stained with anti-IA/IE, mPDCA1, anti-CD8α and anti-CD8β antibodies. CD8α and CD8β surface expression was analyzed by flow cytometry on pDCs gated according to mPDCA1 and IA/IE staining. Gates were set based on isotype controls, numbers in outlined areas indicate the percentage of positive cells in the designated region. Representative dot plots from five experiments are shown. **(b)** Plasmacytoid DCs magnetically purified from peripheral lymph nodes of naïve mice were stained with mPDCA1, anti-IA/IE or anti-CD11c along with CD8α and CD8β antibodies and analyzed by fluorescence confocal microscopy. Original magnification x1000. **(c)** Percentage of $CD8\alpha^{-}\beta^{-}$, $CD8\alpha^{+}\beta^{-}$ and $CD8\alpha^{+}\beta^{+}$ pDCs in peripheral lymph nodes, spleen, lungs, blood and thymus. Data are from two independent experiments (mean ± SEM). **(d)** Surface expression of Siglec-H, Ly6c, B220, Ly49Q, IA/IE, CD80, CD86, CD40, PD-L1, PD-L2, ICOS-L and OX40-L was assessed by flow cytometry on $CD8\alpha^{-}\beta^{-}$ pDCs, $CD8\alpha^{+}\beta^{-}$ pDCs and $CD8\alpha^{+}\beta^{+}$ pDCs from peripheral lymph nodes. Shaded histograms represent isotype control antibodies; solid black lines specific stainings. Data are representative of three independent experiments.

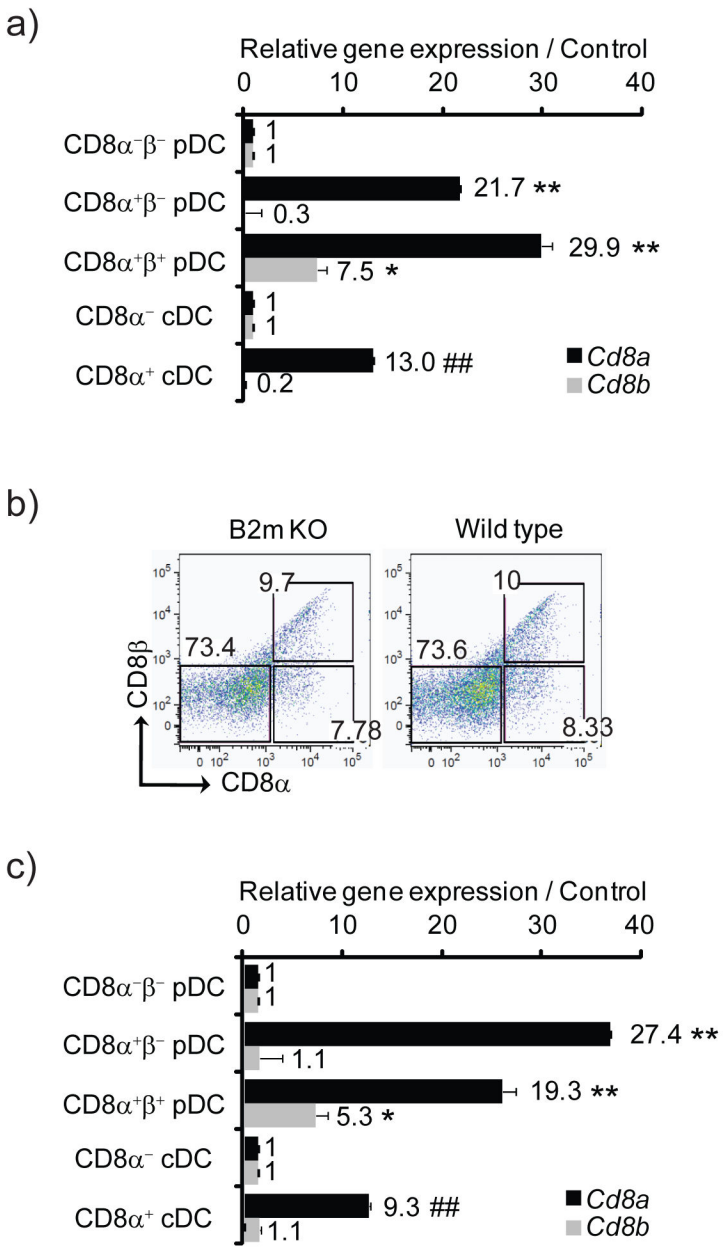

Figure 2. CD8α and CD8β are co-expressed on a subset of pDCs but not on cDCs

(a) $CD8\alpha^{-}\beta^{-}$, $CD8\alpha^{+}\beta^{-}$ and $CD8\alpha^{+}\beta^{+}$ pDCs from peripheral lymph nodes or splenic $CD8\alpha^{-}$ and $CD8\alpha^{+}$ cDCs were sorted by flow cytometry from Flt3-L-treated mice before isolation of total RNA. Relative gene expression of *Cd8a* and *Cd8b* genes was assessed by quantitative real-time PCR. $CD8\alpha^{-}\beta^{-}$ pDCs were used as a calibrator to evaluate *Cd8a* and *Cd8b* gene expression in $CD8\alpha^{+}\beta^{-}$ and $CD8\alpha^{+}\beta^{+}$ pDCs while $CD8\alpha^{-}$ cDCs served as a reference to measure *Cd8a* and *Cd8b* gene expression in $CD8\alpha^{+}$ cDCs. Data are the average ± SEM of six independent experiments. **(b)** CD8α and CD8β surface expression was assessed by flow cytometry in $B2m^{-/-}$ mice lacking $CD8^{+}$ T cells. Plasmacytoid DCs from pooled peripheral lymph nodes of Flt3-L-treated WT or $B2m^{-/-}$ mice, were stained with

CD8α and CD8β specific antibodies and analyzed by flow cytometry. Gates were defined using isotype controls and numbers in outlined areas represent the percentage of positive cells for each population. Data are representative of two experiments. **(c)** Expression of *Cd8a* and *Cd8b* genes was tested by real-time PCR in $CD8\alpha^{-}\beta^{-}$, $CD8\alpha^{+}\beta^{-}$ and $CD8\alpha^{+}\beta^{+}$ pDCs or splenic $CD8\alpha^{-}$ and $CD8\alpha^{+}$ cDCs isolated by cell sorting from Flt3-L-treated $B2m^{-/-}$ mice. Data are the mean ± SEM of three different experiments. P values were calculated with Student's t-test. *: p value < 0.05, **: p value < 0.02 (compared to $CD8\alpha^{-}\beta^{-}$ pDCs). ##: p value < 0.02 (compared to $CD8\alpha^{-}$ DCs).

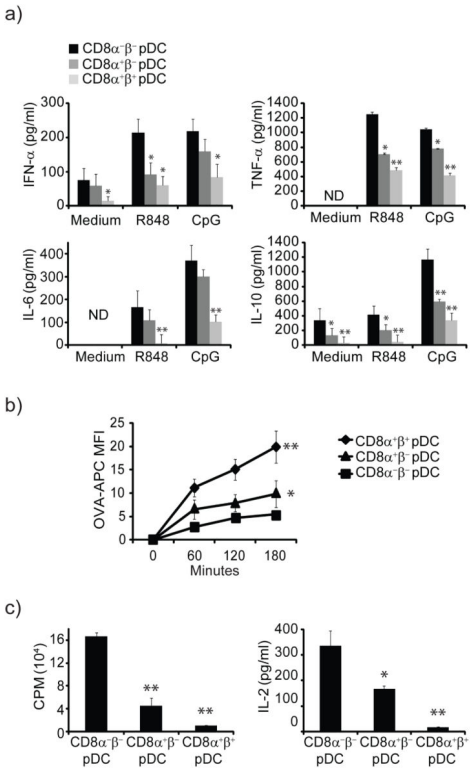

Figure 3. CD8α$^+$β$^-$ and CD8α$^+$β$^+$ pDCs produce low amount of cytokines and weakly prime naïve CD4$^+$ T cells

(a) Plasmacytoid DCs subsets were sorted by flow cytometry from peripheral lymph nodes of mice treated with Flt3-L according to their expression of CD8α or CD8αβ. CD8α$^-$β$^-$, CD8α$^+$β$^-$ and CD8α$^+$β$^+$ pDCs were subsequently stimulated *in vitro* with R848 (1 μg/ml) or CpG (1 μM) for 24 hours. Culture supernatants were tested for IFN-α, IL-6, TNF-α and IL-10 by ELISA. Results are average ± SEM of two independent experiments. **(b)** Plasmacytoid DCs subsets were cultured for 60, 120 or 180 minutes in presence of OVA-APC (10 μg/ml) at 37°C or 4°C. Cells were then washed and stained with CD8α and CD8β antibodies. APC fluorescence was analyzed by flow cytometry in CD8α$^-$β$^-$, CD8α$^+$β$^-$ or CD8α$^+$β$^+$ pDCs subpopulations. Data are average of [(mean fluorescence intensity (MFI) at 37°C) – (MFI at 4°C)] ± SEM of three separate experiments. **(c)** Naïve CD4$^+$ T cells from DO11.10 mice were co-cultured with CD8α$^-$β$^-$, CD8α$^+$β$^-$ or CD8α$^+$β$^+$ pDCs. Cells were cultured for three days at a 1:10 ratio (pDCs: CD4$^+$ T cells) with 10 μg/ml of OVA before being pulsed for 18 hours with ^{3}H thymidine. Incorporation of radioactivity was determined by liquid scintillation counting. Alternatively, supernatants were collected and tested for IL-2 by ELISA. Results are the mean of triplicates ± SEM of one representative experiment out of two. P values were determined using the Student's t-test. *: p value < 0.05, **: p value < 0.02 (compared to CD8α$^-$β$^-$ pDCs).

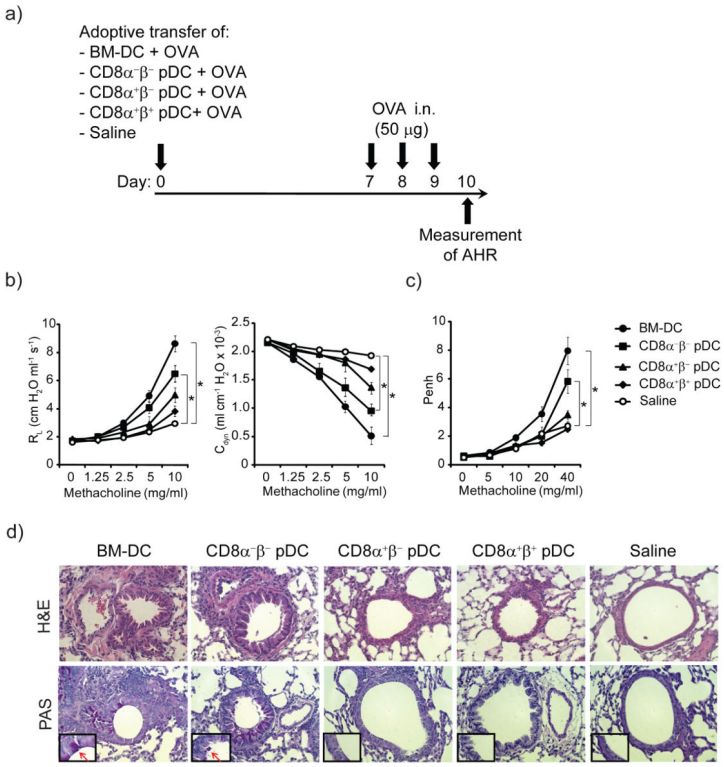

Figure 4. CD8α$^-$β$^-$ pDCs promote the development of airway hyperreactivity

(a) Plasmacytoid DCs subsets isolated by cell sorting from peripheral lymph nodes of Flt3-L-treated mice or BM-DCs were loaded with OVA (10 µg/ml) for 4 hours then adoptively transferred into naïve BALB/c mice (2×10^5 cells per mice). Seven days later, mice were challenged by intranasal administration of OVA (50 µg in 50 µl PBS) on three consecutive days. **(b)** Airway hyperresponsiveness was subsequently assessed by plethysmography to measure lung resistance (R_L), dynamic compliance (C_{dyn}) and **(c)** enhanced pause (Penh). Data are average ± SEM of groups of 5 mice of one representative experiment out of two. *: $p < 0.05$ as determined by two-tailed Student's t-test. **(d)** Representative lung histology of mice from panel (c). Lung tissue from mice transferred with CD8α$^-$β$^-$ pDCs, CD8α$^+$β$^-$ pDCs, CD8α$^+$β$^+$ pDCs or BM-DCs were stained with hematoxylin and eosin (H&E, upper panel) and periodic acid Schiff (PAS, lower panel). Arrows show the release of the mucus in the lumen. Original magnification x200, inset x600.

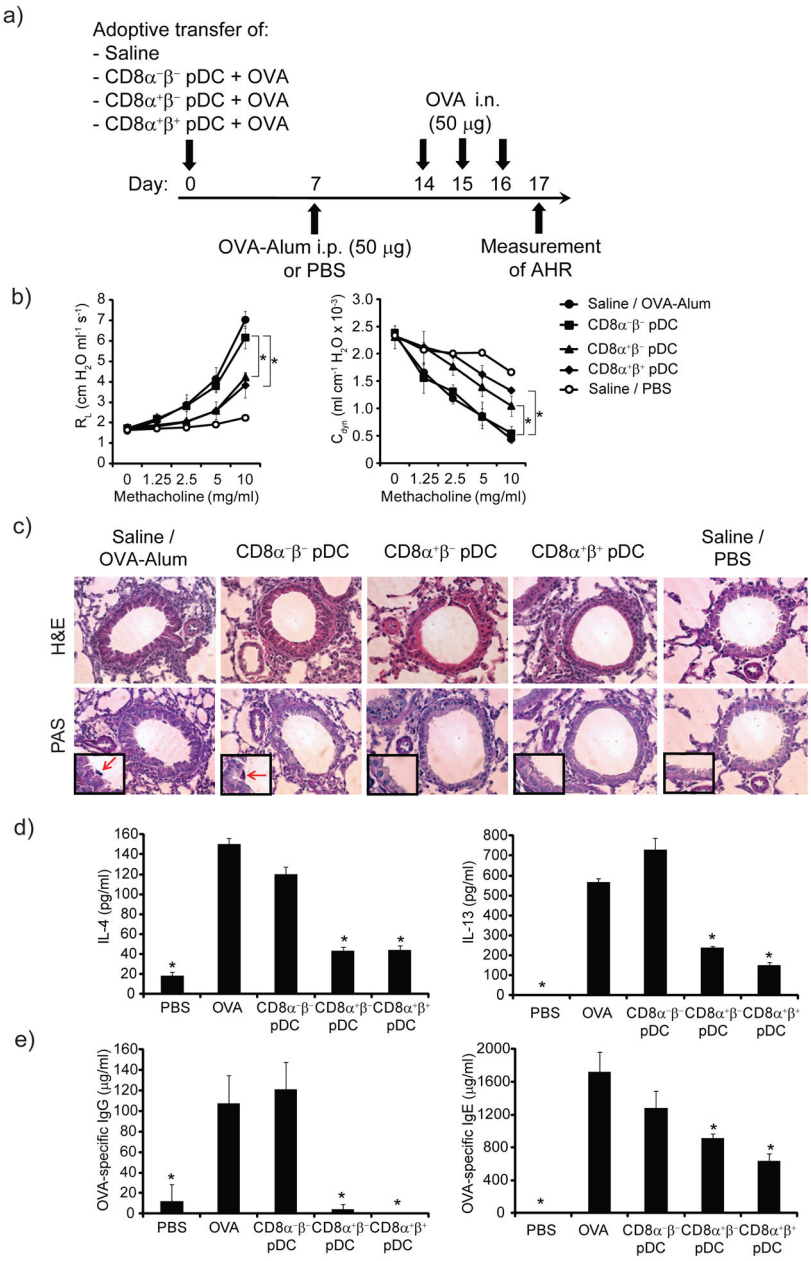

Figure 5. CD8α⁺β⁻ and CD8α⁺β⁺ pDCs prevent the development of airway hyperreactivity

(a) CD8α⁻β⁻, CD8α⁺β⁻ and CD8α⁺β⁺ pDCs sorted by flow cytometry from peripheral lymph nodes of Flt3-L-treated mice were loaded with OVA (10 μg/ml) for 4 hours. Cells were then adoptively transferred into naïve BALB/c mice (2×10^5 cells per mice). At day 7, mice were immunized by intra-peritoneal injection of OVA (50 μg) in Alum (2 mg) and challenged at days 14, 15 and 16 by intranasal administration of OVA (50 μg in 50 μl saline). **(b)** At day 17, airway hyperresponsiveness was assessed by measurement of lung resistance and dynamic compliance by invasive plethysmography. Results are the mean ± SEM of 5 mice groups of one representative experiment out of two. *: $p < 0.05$ as calculated with the Student's t-test **(c)** Representative lung histology of mice from panel (b). Lung

tissue from mice transferred with $CD8\alpha^{-}\beta^{-}$, $CD8\alpha^{+}\beta^{-}$ and $CD8\alpha^{+}\beta^{+}$ pDCs or saline were stained with H&E (upper panel) and PAS (lower panel). Arrows show the release of the mucus in the lumen (Original magnification x200, inset x600). (d) A suspension of lung cells was prepared after enzymatic digestion of lungs and isolation of leukocytes by density gradient centrifugation and positive selection using CD45 microbeads. Lung leukocytes were then plated and restimulated with OVA (100 μg/ml) for 3 days. Culture supernatants were harvested and tested for IL-4 and IL-13 by ELISA. (e) Sera were collected on day 17 and OVA-specific IgE and IgG levels were determined by ELISA. *: $p < 0.05$ compared to OVA-sensitized mice (OVA).

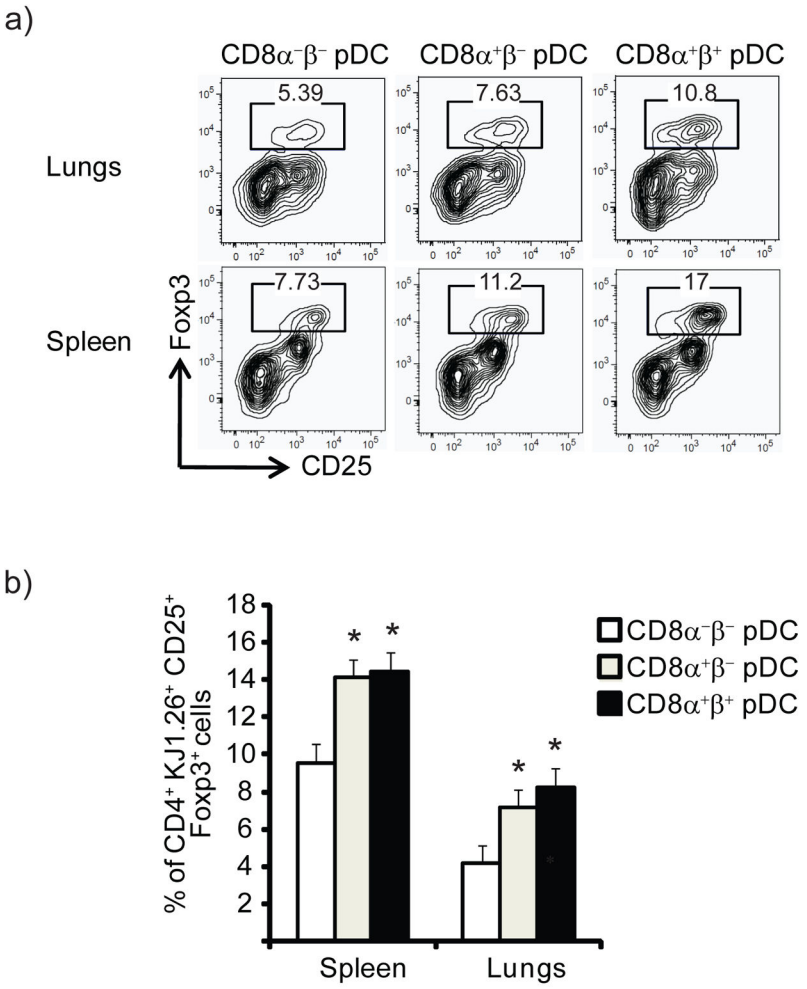

Figure 6. CD8α$^+$β$^-$ and CD8α$^+$β$^+$ pDCs promote the conversion of naïve CD4$^+$ T cells into CD4$^+$ CD25$^+$ Foxp3$^+$ T cells *in vivo*

(a) Plasmacytoid DCs subsets were sorted from peripheral lymph nodes of Flt3-L-treated mice, loaded with OVA (4 hours in presence of 10 μg/ml of OVA) and co-transferred by intravenous injection with naïve OVA-specific CD4$^+$ T cells (3×10^5 pDCs and 3×10^6 CD4$^+$ CD62L$^+$ Foxp3$^-$ T cells) into naïve BALB/c mice. Four days later, mice were challenged by intranasal administration of OVA (50 μg in PBS). At day 5, spleen and lung were harvested and expression of Foxp3 was analyzed in individual mouse by flow cytometry in CD3$^+$ CD4$^+$ KJ1.26$^+$ CD25$^+$ cells. Results shown are representative dot plots and **(b)** mean ± SEM of two independent experiments performed with groups of three mice. *: $p < 0.05$ as calculated with the Student's t-test.

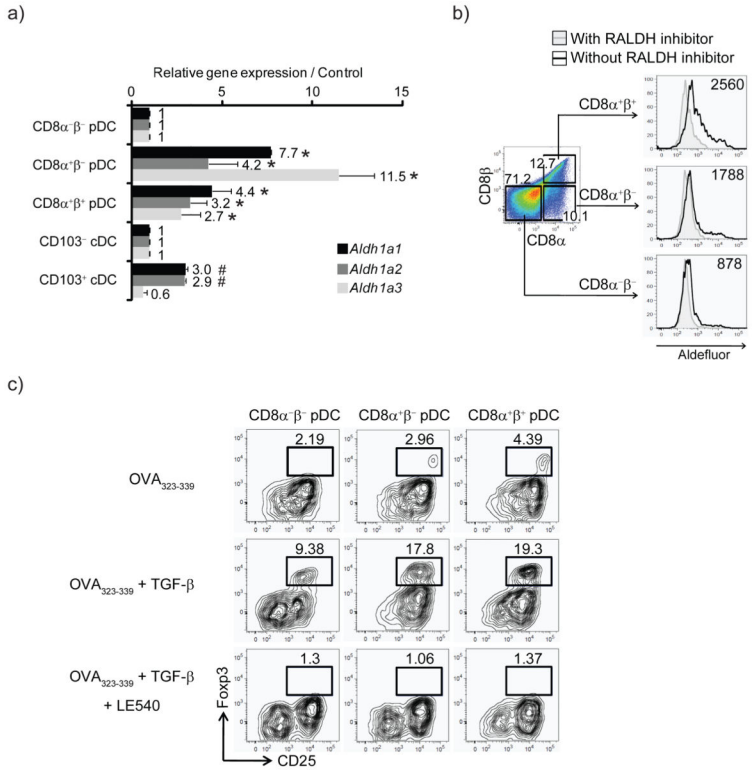

Figure 7. CD8α$^+$β$^-$ and CD8α$^+$β$^+$ pDCs exhibit high RALDH activity and promote the differentiation of CD4$^+$ CD25$^+$ Foxp3$^+$ T cells *in vitro* in a TGF-β and retinoic acid dependent manner

(a) Gene expression of *Aldh1a1*, *Aldh1a2* and *Aldh1a3* was assessed by real-time PCR in CD8α$^-$β$^-$, CD8α$^+$β$^-$ and CD8α$^+$β$^+$ pDCs from peripheral lymph nodes or in CD103$^-$ and CD103$^+$ DCs from mesenteric lymph nodes of Flt3-L-treated mice. Data are mean ± SEM of two independent experiments. **(b)** Plasmacytoid DCs were incubated for 45 minutes at 37°C in presence of Aldefluor substrate with or without diethylaminobenzaldehyde (DEAB, RALDH inhibitor) to determine background staining. Cells were subsequently stained with anti-CD11c, anti-mPDCA1, anti-CD8α and anti-CD8β antibodies and analyzed by flow cytometry in order to detect RALDH activity. Histograms are representative of three independent experiments with MFI values indicated. **(c)** Naïve OVA-specific CD4$^+$ T cells were cultured with CD8α$^-$β$^-$, CD8α$^+$β$^-$ or CD8α$^+$β$^+$ pDCs at a 1:10 ratio (pDC:T CD4$^+$) for five days in presence of OVA$_{323-339}$ peptide with or without TGF-β (1 ng/ml) or LE540 (1 μM) as indicated. Cells were subsequently stained with CD3, CD4 and CD25 antibodies, fixed, permeabilized and stained for intracellular Foxp3 prior to flow cytometry analysis. Foxp3 expression was analyzed among CD3$^+$ CD4$^+$ CD25$^+$ cells, dot plots are representative of three independent experiments.